

Jordan Journal of Physics

ARTICLE

Effect of the Electrode Bore Angle on the Two-Electrode Electrostatic Immersion Lens Design

M. A. Al-Khashab and A. I. M. Al-Abdullah

Physics Department, College of Science, Mosul University, Mosul, Iraq.

Received on: 27 / 6 / 2012; Accepted on: 30 / 10 / 2012

Abstract: This paper describes the influence of the front electrode bore angle on the electron optical performance of the two-electrode electrostatic immersion lens. The electrode bore shape is the most important geometrical parameter in any electron optical device. Accordingly, a design of an electrostatic immersion lens is presented and its electron optical properties are calculated and compared for different values of bore angle of the electrode facing the incident electron beam. It has been found that the electrode bore angle has a slight effect on the electron optical properties of the electrostatic lens design. Moreover, the best compromise aberration coefficients are obtained at an angle equal to (16°).

Keywords: Electrostatic lens design; Electrostatic immersion lens; Electron optical properties.

Introduction

Electrostatic lenses are used for the extraction, focusing, deceleration and acceleration of electron and ion beams. They are of great importance in the design of low energy electrostatic accelerators such as Cockcroft-Walton and Van de Graff accelerators [1]. Recently, add-on immersion electrostatic-magnetic lens attachments have been designed to improve the resolution of conventional scanning electron microscopes (SEMs) which can acquire images with a resolution of better than 4 nm at a landing energy of 600 eV [2].

The theory of electrostatic lenses has been developed in the early 1930s. The solution of the paraxial ray equation and the introduction of the matrix formalism are illustrated in [3, 4]. The solution of the paraxial ray equation at relativistic energies can be found in [5, 6]. Ion optics with rotationally symmetric electrostatic lenses is presented in [1]. Accurate and extensive data calculation on the objective focal properties and the third-order aberrations of electrostatic lenses can be found in [7, 8]. Progress in the calculation of electron optical properties in

recent years have been reviewed in [9, 10] and especially in [11].

Intensive studies have been rigorously carried out to optimize the geometrical structure and the dimensions of electrostatic lenses. New models of asymmetrical electrostatic immersion lenses have been introduced in [12]. An electrostatic einzel lens fabricated using micro-fabrication technology is described in [13]. The design and fabrication of cylindrical multi-element electrostatic lenses at the nanoscale down to 140 nm in aperture diameter and 4.2 μm in column length are presented in [14].

In this research work, we study the effect of front electrode bore angle of a two-electrode electrostatic immersion lens on its electron optical properties.

Design Considerations

The cross-section of the prototype electrostatic immersion lens as well as its geometrical parameters and shape dimensions are shown in Fig. 1. In the proposed design, the

voltage applied to the front electrode of truncated conical-shaped bore, facing the incident electron, is denoted by (V_1). The second electrode, facing the image side, has a cylindrical bore; the applied voltage is denoted by (V_2). The bore diameters of the two electrodes, denoted by (D_1) and (D_2), are equal to 4 mm and 6 mm, respectively [15]. The bore angle of the first electrode is denoted by (θ). The space between the two electrodes, denoted by (L), is 10 mm.

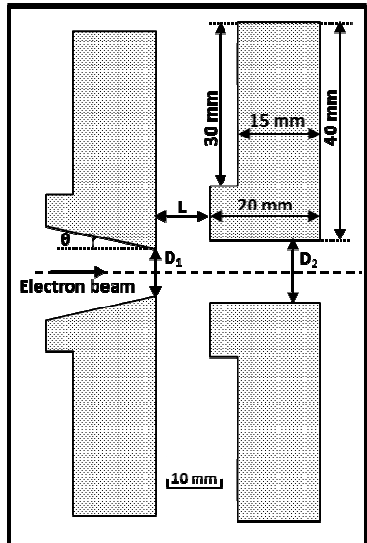


FIG. 1. Cross-section of the electrostatic immersion lens design with its geometrical parameters and dimensions

$$C_{si} = \frac{1}{16 V_i^{\frac{1}{2}} r_i^4} \int_{Z_o}^{Z_i} \left\{ \left[\frac{5}{4} \left(\frac{V''}{V} \right)^2 + \frac{5}{24} \left(\frac{V'}{V} \right)^4 \right] r^3 + \frac{14}{3} \left(\frac{V'}{V} \right)^4 r'^3 r^3 - \frac{3}{2} \left(\frac{V'}{V} \right)^2 r'^2 r^2 \right\} V^{\frac{1}{2}} dz$$

$$C_{ci} = \frac{V_i^{\frac{1}{2}}}{r_i^2} \int_{Z_o}^{Z_i} \left(\frac{V'}{2V} r' r + \frac{V''}{4V} r^2 \right) V^{-\frac{1}{2}} dz$$

where (C_{si}) and (C_{ci}) are the spherical and the chromatic aberration coefficients, respectively, at the image plain, (Z_o) and (Z_i) are the object and image plane positions, respectively, (V_i) is the potential at the image plain, (V') and (V'') are the first and second derivatives of the axial potential, (r) is the electron trajectories and (r_i') is the slope of the electron trajectories at each point which can be found using the following paraxial ray equation:

$$r''(Z) + \frac{V'}{2V} r'(Z) + \frac{V''}{4V} r(Z) = 0$$

The above equation can be solved numerically using the “fourth-order Range-Kutta” method [18].

Procedure and Results

In order to determine the best bore angle for the front electrode of the two-electrode electrostatic immersion lens, the electron optical properties are calculated and compared systematically using constant electrode voltage at the same “finite magnification condition” of operation [16]. The calculation is accomplished by using a modified version of some Munro’s programs [16]. The modification made in this research work involves enhancing the fine and coarse mesh numbers in the axial and radial directions. More accurate finite element calculations are necessary for handling the complicated shape design [17]. Moreover, the programs have been modified to calculate and illustrate the electron trajectories inside the lens structure.

The spherical aberration coefficient C_s and the chromatic aberration coefficient C_c are considered as the best criteria for the comparison between the optical instruments [8]. These coefficients can be calculated numerically from the following non-relativistic formula using Simpson’s rule [19]:

The calculation of the electron optical properties is completed under the same operational condition of applied voltages ($V_1 = 100$ V) and ($V_2 = 3$ kV) and using the “finite magnification condition” with object plain position (Z_o) equal to 114 mm [15]. In this research work, we consider the previous parameters as constant values in the calculation of the electron optical properties. The values of the first electrode bore angle have been chosen equal to (0, 5, 11, 16 and 21)°.

The axial potential distribution is calculated for each value of the bore angle and compared in Fig. 2. The Figure shows the axial potential profile curves at the location of the front electrode. These curves rise more rapidly as the bore angle increases.

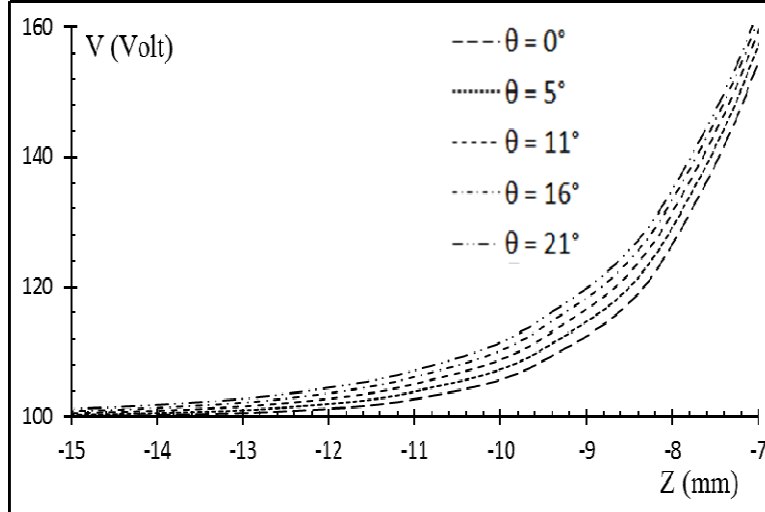
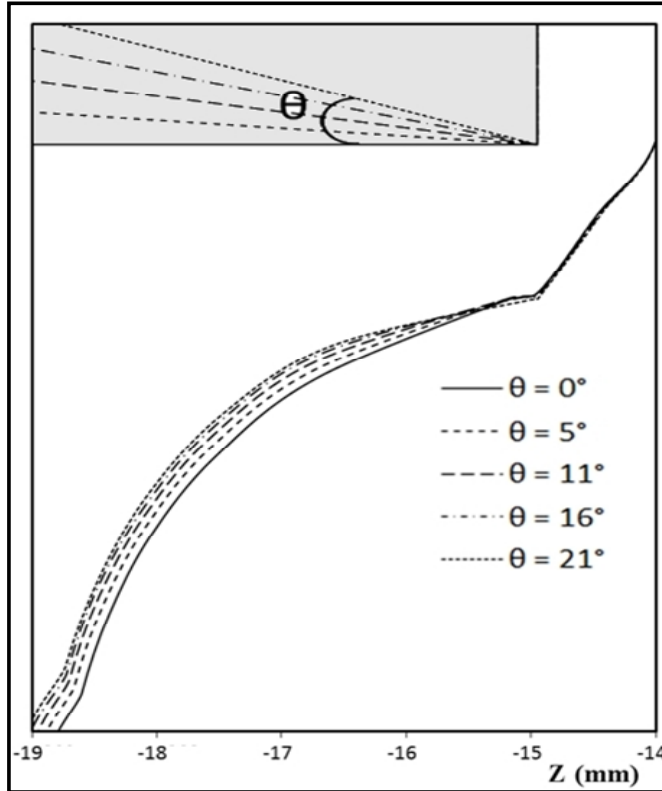


FIG. 2. Variation of the axial potential distribution due to the variation of the electrode bore angle


 FIG. 3. Variation of the front electrode closest equipotential line trajectories with its bore angle θ

The variations of the single equipotential line with the front electrode bore angle are illustrated in Fig. 3. This Figure shows that the shift of the equipotential line inside the electrode bore becomes greater as the electrode bore angle increases. The differences between the equipotential line trajectories are more noticeable at the small values of the bore angle compared to those at the larger values of the bore

angle. As a result, a larger angle produces a stronger stray field inside the bore.

The electron beam trajectories have also been calculated for each value of bore angle. Fig. 4 shows a comparison of the electron trajectories at the cross-over point for different values of the bore angle. The Figure shows that the cross-over points are shifted toward the image side as the bore angle increases (i.e., as the focal length increases).

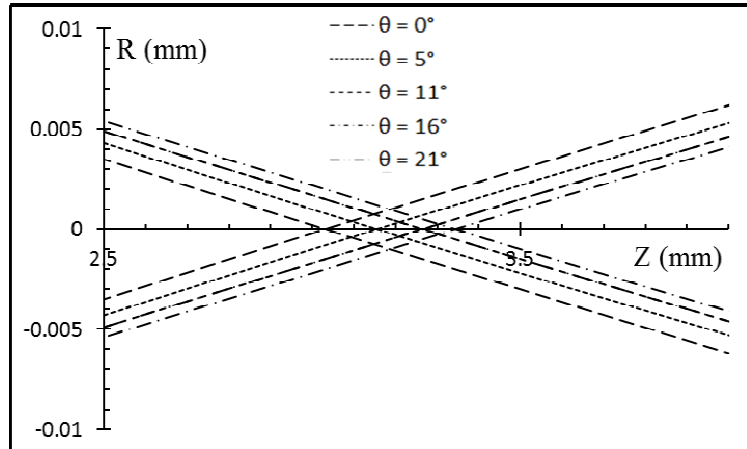


FIG. 4. Variation of the electron trajectories profile at the cross-over points due to the variation of the electrode bore angle

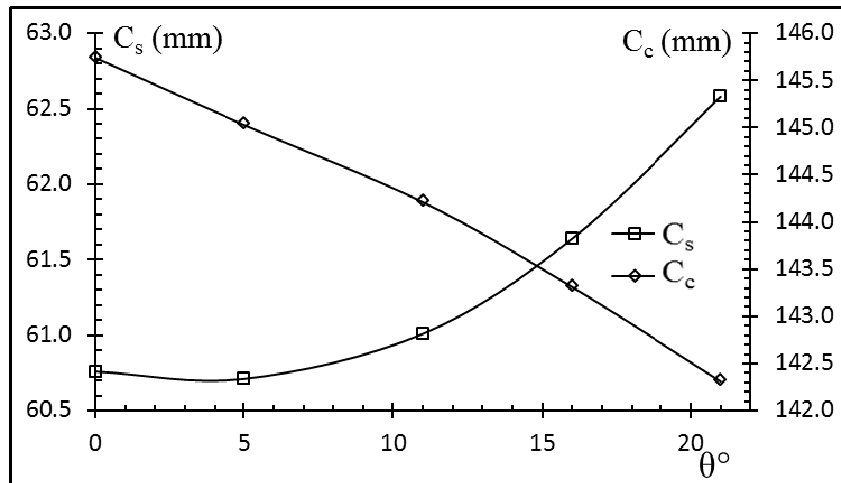


FIG. 5. Variation of the spherical and chromatic aberration coefficients due to the variation of the electrode bore angle

The spherical and the chromatic aberration coefficients are calculated for the same range of electrode bore angles and compared with each other as shown in Fig. 5. The calculation is carried out at the same electrodes voltage ($V_1 = 100$ V and $V_2 = 3kV$). The object plain position equals ($Z_o = 114$ mm) at the “finite magnification condition”. Fig. 5 shows that the spherical aberration coefficient increases as the value of the bore angle increases, while the chromatic aberration coefficient decreases. Accordingly, we can consider that the best compromise aberration coefficients are obtained at an angle of (16°).

Conclusions

We study the front-electrode bore angle for a new design of immersion electrostatic lens different from the planar-apertured and tubular electrode configurations. It has been found that the electrode bore angle has a slight effect on the electron optical properties of the electrostatic lens design. The spherical aberration coefficient increases as the value of the bore angle increases, while the chromatic aberration coefficient decreases. The best compromise aberration coefficients are obtained at an angle of 16° . Larger angles produce more stray field inside the bore. The difference between two successive equipotential line trajectories decreases when the value of the bore angle increases.

References

- [1] Hinterberger, F., "The Physics of Particle Accelerators", Ch. 4 and 5, (Springer-Verlag, Berlin, Heidelberg, New York, 2005).
- [2] Khursheed, N. and Karuppiah, N., American Inst. of Phys., 73(8) (2002) 2906.
- [3] Septier, A., "Applied Charged Particle Optics", (ACADEMIC PRESS, INC. 24/28 Oval Road, London NW1 7DX., 1980).
- [4] Liebl, H., "Applied Charged Particle Optics", Ch.2-4, 45-104, (Springer, 2008).
- [5] Zworykin, V.K., Morton, G.A., Ramberg, E.G., Hillier, J. and Vance, A.W., "Electron Optics and the Electron Microscope", (Wiley, New York, 1945).
- [6] Lawson, J.D., "The Physics of Charged Particle Beams", Ch.5, 161-201, (Clarendon Press, Oxford, 1988).
- [7] Grivet, P., "Electron Optics", Ch.4, 85-119, (Pergamon Press, London. Part 1, 1965).
- [8] Hawkes, P.W. and Kasper, E., "Principles of Electron Optics", Part 2, Ch.35, (ACADEMIC PRESS, Inc., 629-686, 1996).
- [9] Hawkes, P.W., Annales de la Fondation Louis de Broglie, 29(1) (2004) 837.
- [10] Sise, O., Ulu, M. and Dogan, M., Nucl. Instrum. Methods A., 54 (2005) 114.
- [11] Lencová, B., Electrostatic Lenses, in: "Handbook of Charged Particle Optics", (J. Orloff, Ed.), (CRC Press, Boca Raton, 161–208, 2009).
- [12] Al-Khashab, M.A. and Al-Shamma, M.T., Dirasat, Pure Sciences, 36(2) (2009) 171.
- [13] Syms, R.R.A., Michelutti, L. and Ahmad, M.M., Sensors and Actuators, A107 (2003) 285.
- [14] Sinno, I., Sanz-Velasco, A., Kang, S., Jansen, H., Olsson, E., Enoksson, P. and Svensson, K., Journal of Micromechanics and Microengineering, 20(9) (2010) 095031.
- [15] Al-Khashab, M.A. and Al-Abdullah, A.I.M., Rafidain Journal of Science, (2013), Unpublished.
- [16] Munro, E., "A Set of Computer Programs for Calculating the Properties of Electron Lenses", Report CUED/B-ELECT/TR 45. Cambridge University, Eng. Dept. (1975).
- [17] Orloff, J., "Handbook of Charged Particle Optics", Ch.1, 3-11. (CRC Press LLC, 1997).
- [18] Hawkes, P.W., "Electron Optics and Electron Microscopy", Ch.2, 27-44. (Taylor and Francis, Ltd., London, 1972).
- [19] Szilagyi, M. and Szep, J., J. Vac. Sci. Technol., B6 (1988) 953.